MEDIC-2F: A One-Dimensional Diffusive Mixing Model Application to LMJ Target Simulations

François RENAUD and Denis SOUFFLAND

Commissariat à l'Énergie Atomique
DAM/Île-de-France
B.P. 12
91680 Bruyères-le-Châtel
FRANCE

françois.renaud@cea.fr and denis.souffland@cea.fr

1. Introduction

In laser-driven explosion experiments, a degradation of the single shell capsule yield is forecast due to the mixing between the fuel and the shell. This mixing is induced by the growth of hydrodynamic instabilities at the interface. These processes have various origins (inner and outer shell roughness, laser drive perturbations, …) and evolve through different ways (Rayleigh-Taylor and Richtmyer-Meshkov instabilities, "feed-through", …). The numerical simulations of these intrinsically three-dimensional phenomena are still costly in term of cpu-time. We thus need a one-dimensional model if we want to asses the impact of variations in the definition of the target, the holraum or the laser drive with a moderate cpu-time cost.

The main hypothesis of our one-dimensional model of mixing is that the plasma interpenetration is multifluid and that mass fraction evolution and thermal exchanges could be modelled by means of diffusive processes. An additional diffusive equation calculates the mass fraction evolution of one component of the mixing. The diffusion coefficient depends on the mixing zone length that has to be known from experimental data or from post-processing 2D or 3D computation results. One part of the thermal exchanges is due to the enthalpy exchanged by mass transport. Another part is due to electronic and ionic thermal conduction. All others thermal homogenisation phenomena (energy loss by transverse thermal conduction, 1D averaging, …) are modelled by an effective thermal conduction.

We will show comparisons between our one-dimensional computation results using MEDIC-2F and the 1D-averaging corresponding two-dimensional computation results obtained with the CEA hydrocode FCI2.

2. 1D Diffusive Model (Hydrodynamics)

The interpenetration of the ablator with the fuel is described by a 1D two-fluid mixing model. We have used the model proposed by Saurel *et al*[1].:

- Interface transport equation

$$\frac{D\alpha}{Dt} + (W_{\text{int}} - U)\frac{\partial \alpha}{\partial r} = \mu\left(P_1 - P_2\right), \tag{1}$$

- Mass equations

$$\rho \frac{D}{Dt}\left(\frac{1}{\rho}\right) - \frac{1}{r^d}\frac{\partial}{\partial r}\left(r^d U\right) = 0, \quad \rho \frac{Dc}{Dt} + \frac{1}{r^d}\frac{\partial}{\partial r}\left(r^d \rho c(1-c)\left(u_1 - u_2\right)\right) = 0, \tag{2}$$

- Momentum equations

$$\rho \frac{D}{Dt}\left(\begin{vmatrix} c u_1 \\ (1-c)u_2 \end{vmatrix}\right) + \frac{1}{r^d}\frac{\partial}{\partial r}\left(r^d \begin{vmatrix} \rho c(1-c)\left(u_1 - u_2\right)u_1 \\ -\rho c(1-c)\left(u_1 - u_2\right)u_2 \end{vmatrix}\right) + \frac{\partial}{\partial r}\left(\begin{vmatrix} \alpha P_1 \\ (1-\alpha)P_2 \end{vmatrix}\right) = \begin{vmatrix} + \\ - \end{vmatrix} P_{\text{int}} \frac{\partial \alpha}{\partial r} \begin{vmatrix} + \\ - \end{vmatrix} M_1^{"}, \tag{3}$$

- Total energy equations

$$\rho \frac{D}{Dt}\left(\begin{vmatrix} c E_1 \\ (1-c)E_2 \end{vmatrix}\right) + \frac{1}{r^d}\frac{\partial}{\partial r}\left(r^d \begin{vmatrix} \rho c(1-c)\left(u_1 - u_2\right)E_1 + \alpha P_1 u_1 \\ -\rho c(1-c)\left(u_1 - u_2\right)E_2 + (1-\alpha)P_2 u_2 \end{vmatrix}\right) = \begin{vmatrix} + \\ - \end{vmatrix} P_{\text{int}} W_{\text{int}} \frac{\partial \alpha}{\partial r} \begin{vmatrix} + \\ - \end{vmatrix} M_1^{"} W_{\text{int}} \begin{vmatrix} - \\ + \end{vmatrix} \mu P_{\text{int}}\left(P_1 - P_2\right) + S, \tag{4}$$

with $\rho = \alpha\rho_1 + (1-\alpha)\rho_2$, $c = \frac{\alpha\rho_1}{\rho}$, $U = cu_1 + (1-c)u_2$, $\frac{D.}{Dt} = \frac{\partial.}{\partial t} + U\frac{\partial.}{\partial r}$.

Then the two-fluid flow is split into a mean flow and a relative flow with interface transport:

- Mass equations

$$\rho\frac{D}{Dt}\left(\frac{1}{\rho}\right) - \frac{1}{r^d}\frac{\partial}{\partial r}\left(r^d U\right) = 0,$$

$$\rho\frac{Dc}{Dt} + \frac{1}{r^d}\frac{\partial}{\partial r}\left(r^d \rho c(1-c)(u_1-u_2)\right) = 0, \quad (5)$$

- Momentum equation

$$\rho\frac{DU}{Dt} + \frac{\partial P}{\partial r} + \frac{1}{r^d}\frac{\partial}{\partial r}\left(r^d \rho c(1-c)(u_1-u_2)^2\right) = 0, \quad (6)$$

- Internal energy equation

$$\rho\frac{D\varepsilon}{Dt} + P\frac{1}{r^d}\frac{\partial}{\partial r}\left(r^d U\right) + \frac{1}{r^d}\frac{\partial}{\partial r}\left(r^d \rho c(1-c)(u_1-u_2)(h_1-h_2)\right) + \left(-(1-c)\frac{\partial \alpha P_1}{\partial r} + c\frac{\partial(1-\alpha)P_2}{\partial r} + P_{int}\frac{\partial \alpha}{\partial r} + M_1^{"}\right)(u_1-u_2) = S \quad (7)$$

where $h_{1\text{ or }2}$ is the enthalpy of each fluid. Thus, we need closure relations to describe the relative flow and the interface transport. The mass fraction exchange is modelled by means of a diffusive process:

$$\rho c(1-c)(u_1-u_2) = -\rho D\frac{\partial c}{\partial r}, \quad (8)$$

and we neglect all the momentum and energy exchanges except the enthalpy one:

$$\rho c(1-c)(u_1-u_2)^2 << 1,$$

$$\left(-(1-c)\frac{\partial \alpha P_1}{\partial r} + c\frac{\partial(1-\alpha)P_2}{\partial r} + P_{int}\frac{\partial \alpha}{\partial r} + M_1^{"}\right)(u_1-u_2) << 1 \quad (9)$$

and $\rho c(1-c)(u_1-u_2)(h_1-h_2) = -\rho D\frac{\partial c}{\partial r}(h_1-h_2)$ (10)

We also consider the two fluids in an isothermal and isobaric equilibrium.

To close the interface transport equation we had to express the diffusive coefficient D. Following Souffland and Renaud[2] and Alon and Shvarts[3], a diffusive coefficient in each part of the mixing zone (see Fig. 1) is defined as:

$$D_l = \mathrm{Max}\left(\frac{1}{8\xi^2}L_{mix.,l}\frac{dL_{mix.,l}}{dt}\left(1+\frac{r-R_{int}}{L_{mix.,l}}\right)\left(1-\frac{r-R_{int}}{L_{mix.,r}}\right)\frac{\overline{\rho}_l}{\rho},0\right)$$

$$D_r = \mathrm{Max}\left(\frac{1}{8\xi^2}L_{mix.,r}\frac{dL_{mix.,r}}{dt}\left(1+\frac{r-R_{int}}{L_{mix.,l}}\right)\left(1-\frac{r-R_{int}}{L_{mix.,r}}\right)\frac{\overline{\rho}_r}{\rho},0\right) \quad (11)$$

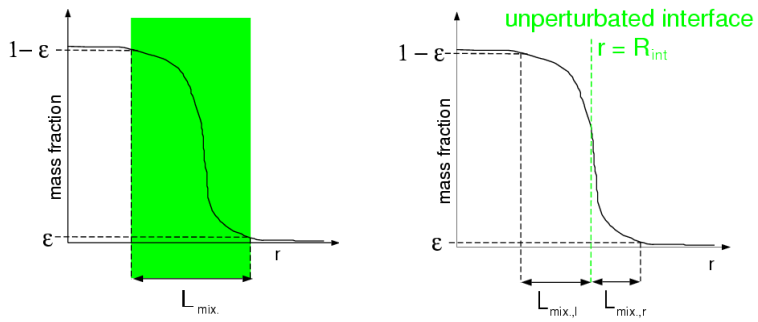

Fig. 1: Description of the mixing zone.

with $\xi = \mathrm{Erf}^{-1}(1-2\varepsilon)$ and where $\overline{...}_{l\text{ or }r}$ is the mean value on the left or right part of the mixing zone (see Fig. 1). The left (right) part of the mixing zone is defined as the part of the mixing zone located on the left (right) side of the unperturbated interface position. We thus need, as data input, the temporal evolution of the mixing lengths $L_{mix,r}$ and $L_{mix,l}$.

3. 1D Diffusive Model (Plasma)

The studied fluids are plasmas with electrons (subscript e) and ions (subscript i) at different temperatures within a photon gas (subscript rad) at its own temperature. The internal energy is now $\varepsilon = \varepsilon_i + \varepsilon_e + E_{rad}/\rho$ and the pressure becomes $P = P_i + P_e + P_{rad}$. Three energy balance equations are written:

- Ionic energy balance

$$\rho\frac{D\varepsilon_i}{Dt} + P_i\frac{1}{r^d}\frac{\partial}{\partial r}\left(r^d U\right) - \frac{1}{r^d}\frac{\partial}{\partial r}\left(r^d \rho \mathcal{D}\frac{\partial c}{\partial r}\left(h_{i,1} - h_{i,2}\right)\right) = \left(\frac{1}{r^d}\frac{\partial}{\partial r}\left(r^d \kappa_i \frac{\partial T_i}{\partial r}\right)\right)^{mix.} + S_{e\leftrightarrow i} + S_{fusion\to i} \qquad \textbf{(12)}$$

- Electronic energy balance

$$\rho\frac{D\varepsilon_e}{Dt} + P_e\frac{1}{r^d}\frac{\partial}{\partial r}\left(r^d U\right) - \frac{1}{r^d}\frac{\partial}{\partial r}\left(r^d \rho \mathcal{D}\frac{\partial c}{\partial r}\left(h_{e,1} - h_{e,2}\right)\right) = \left(\frac{1}{r^d}\frac{\partial}{\partial r}\left(r^d \kappa_e \frac{\partial T_e}{\partial r}\right)\right)^{mix.} - S_{e\leftrightarrow i} - S_{e\leftrightarrow rad} + S_{fusion\to e} \qquad \textbf{(13)}$$

- Radiative energy balance

$$\frac{DE_{rad}}{Dt} + E_{rad}\frac{1}{r^d}\frac{\partial}{\partial r}\left(r^d U\right) + P_{rad}\frac{1}{r^d}\frac{\partial}{\partial r}\left(r^d U\right) = \left(\frac{1}{r^d}\frac{\partial}{\partial r}\left(r^d \kappa_{rad}\frac{\partial T_{rad}}{\partial r}\right)\right) + S_{e\leftrightarrow rad} \qquad \textbf{(14)}$$

Ionic and electronic thermal conduction in the mixing zone are modelled by an equivalent ionic and electronic thermal conduction:

$$\left(\frac{1}{r^d}\frac{\partial}{\partial r}\left(r^d \kappa_i \frac{\partial T_i}{\partial r}\right)\right)^{mix.} = \frac{1}{r^d}\frac{\partial}{\partial r}\left(r^d \kappa_i^{eff}\frac{\partial T_i}{\partial r}\right) \text{ with } \kappa_i^{eff} = \mathrm{f}_i\left(r, c, T_i, \ldots\right)\kappa_i \qquad \textbf{(15)}$$

$$\left(\frac{1}{r^d}\frac{\partial}{\partial r}\left(r^d \kappa_e \frac{\partial T_e}{\partial r}\right)\right)^{mix.} = \frac{1}{r^d}\frac{\partial}{\partial r}\left(r^d \kappa_e^{eff}\frac{\partial T_e}{\partial r}\right) \text{with } \kappa_e^{eff} = \mathrm{f}_e\left(r, c, T_e, \ldots\right)\kappa_e \qquad \textbf{(16)}$$

where κ_i and κ_e are the ionic and electronic thermal conduction coefficients for molecular mixing. The function f_e and f_i take account of

- interfacial transverse thermal loss by conduction[4],
- 1D averaging of the temperatures (ionic and electronic),
- 1D bi-fluid mean thermal conduction (ionic and electronic),
- …

Outside the mixing zone, f_e and f_i are obviously taken equal to one. In the following simulations, two sets of constants for f_e and f_i are tested. We plan to improve the modelling of these functions in forthcoming studies.

4. LMJ Target Simulations: MEDIC-2F vs. FCI2 Simulations

In order to validate our model in the case of the ablator-fuel mixing in LMJ target, we compare MEDIC-2F simulations to FCI2 2D simulations of LMJ targets implosion. We used two FCI2 simulations[5] corresponding to the targets described in Fig. 2 and Tab. 1.

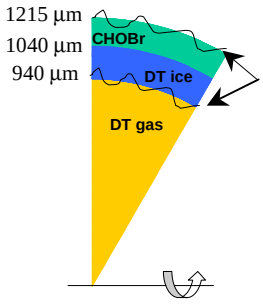

Axi-symetric perturbations
modes 12 to 60

Fig. 2: *Simulated LMJ targets*

Target	Target #1	Target #2
Inner fuel interface perturbations rms	1000 nm	500 nm
Outer ablator interface perturbations rms	50 nm	100 nm

Tab. 1: *Interfaces perturbations rms*

Comparing 2D results with 1D results needs 1D-averaged profiles of the 2D results. The two-phase volume averaging operator[1] is used. We obtain the corresponding density, mass fraction, radial mass centre velocity and pressure FCI2 1D-profiles:

$$\rho_{1D} = \frac{\int_{\upsilon} \rho \, d\upsilon}{\int_{\upsilon} d\upsilon}, \; c_{1D} = \frac{\int_{\upsilon} \rho \chi \, d\upsilon}{\int_{\upsilon} \rho \, d\upsilon}, \; U_{1D} = \frac{\int_{\upsilon} \rho u_{radial} \, d\upsilon}{\int_{\upsilon} \rho \, d\upsilon}, \; P_{1D} = \frac{\int_{\upsilon} P \, d\upsilon}{\int_{\upsilon} d\upsilon}, \qquad \textbf{(17)}$$

where χ is the fuel presence indicator. Furthermore, the 1D mass fraction profile allows us to calculate the mixing lengths $L_{mix,r}$ and $L_{mix,l}$ defined in Fig. 1 and used in the diffusive coefficient expression Eq. 11. So we obtain, as data inputs, the following mixing lengths corresponding to the FCI2 simulations of target #1 and #2:

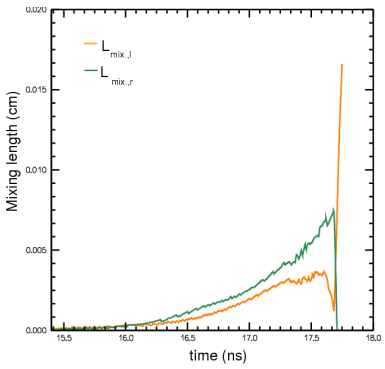

Fig. 3: *Target #1 - mixing lengths $L_{mix,r}$ and $L_{mix,l}$*

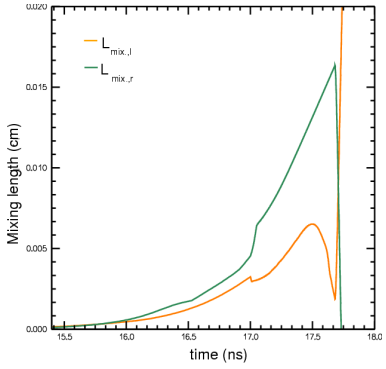

Fig. 4: *Target #2 - mixing lengths $L_{mix,r}$ and $L_{mix,l}$*

We also need to know the value of the constant functions f_e and f_i that characterize (using Eq. 15 and 16) the mixing electronic and ionic thermal conductions. We try two sets of constants: $\{f_i = f_e = 1\}$ and $\{f_e = 25, f_i = f_e^4\}$. The former set was determined after a rough study of the thermal conductive fluxes calculated during the FCI2 simulations.

The results of the comparison are summed up in the figures 5 to 8. For the two simulations, the hydrodynamic profiles (density, mass fraction, radial mass centre velocity and pressure) are in good agreement with the 1D-averaged FCI2 results.
For the yield, the agreement depend on the value of the constant functions f_e and f_i. In the case of the first set of constants, which consider that the mixing thermal conductivities are the molecular mixing ones, the YOC value is overestimated. Using the second set of constants we retrieve the good estimate of YOC for both targets. So thermal homogenisation processes due to the inhomogeneous mixing seem to be strongly involved in the decrease of the yield (see Fig. 8).

5. Conclusions

A one-dimensional diffusive mixing model has been proposed. This model needs only the temporal evolution of the mixing length and the expression of the mixing thermal conductivities. Knowing these data, MEDIC-2F can simulate a LMJ target with high modes perturbations within ~1 h cpu. The model has been validated versus 2D FCI2 simulations of LMJ targets.

Improving the modelling of ionic and electronic thermal conductivities in the mixing zone and in-lining the simulation of the mixing lengths would increase the predictive ability of MEDIC-2F model.

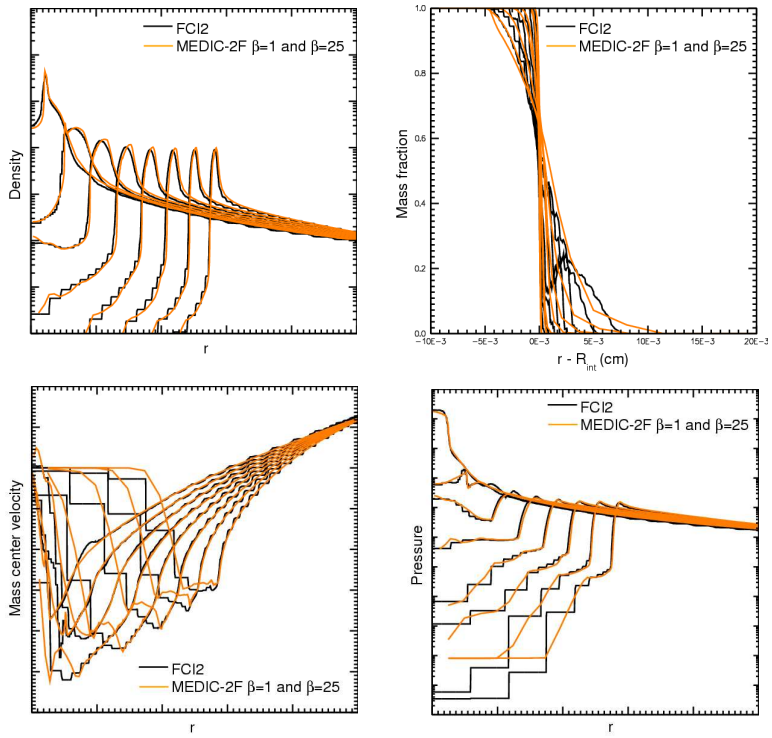

Fig. 5: *Target #1 - Density, mass fraction, radial velocity and pressure profiles at different times from 16.2 ns to 17.6 ns each 0.2 ns.*

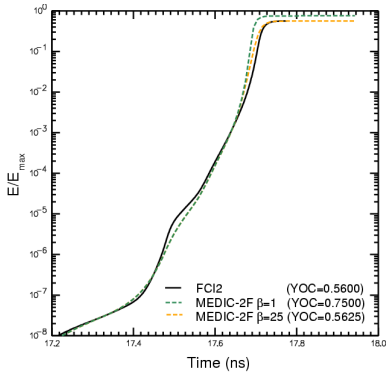

Fig. 6: *Target #1 - temporal evolution of YOC*

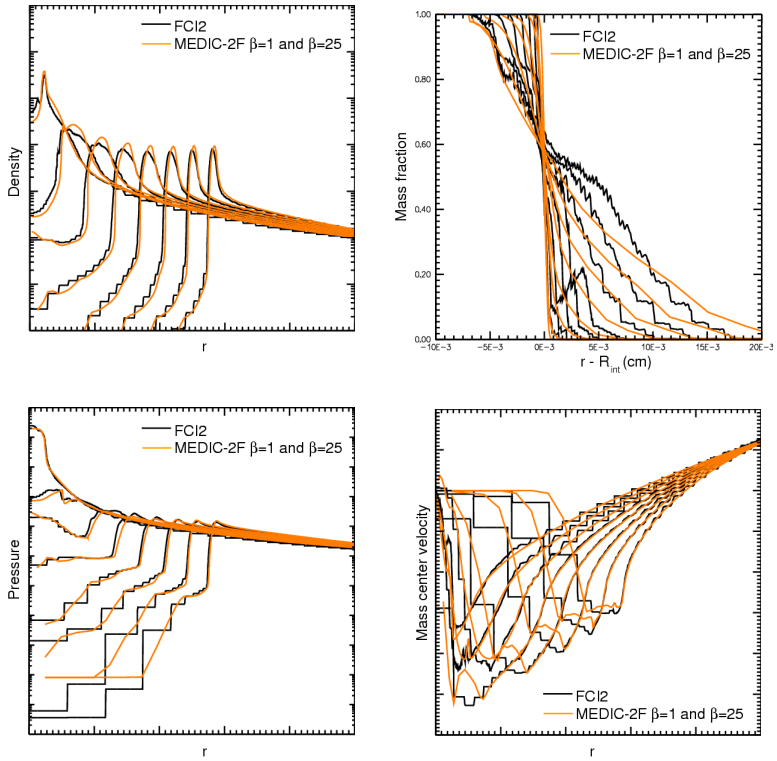

Fig. 7 : *Target #2 - Density, mass fraction, radial velocity and pressure profiles at different times from 16.2 ns to 17.6 ns each 0.2 ns.*

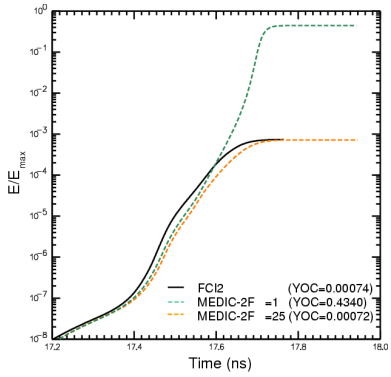

Fig. 8: *Target #2 - temporal evolution of YOC*

References

[1] Gavrilyuk S. and Saurel R. 2002, Mathematical and numerical modelling of two-phase compressible flows with micro-inertia. *J. Intl Computat. Phys.* **175**, pp. 326-360.

[2] Souffland D. and Renaud F. 2001, A Mix-Model for One-Dimensional Simulations of Laser-Driven Implosion Experiments, *in proceedings of the 8th International Workshop on the Physics of Compressible Turbulent Mixing,* Pasadena, USA, December 9-14, 2001

[3] Alon U. and Shvarts D. 1996, Two-phase flow model for Rayleigh-Taylor and Richtmyer-Meshkov mixing, *in proceedings of the 5th International Workshop on the Physics of Compressible Turbulent Mixing,* Stony Brook, USA, July 18-21, 1995, edited by Young R., Glimm J. and Boston B. (World Scientific Publishing).

[4] Juraszek, D. 1993, FCI par laser: Physique de l'implosion, *La fusion thermonucléaire inertielle par laser* ***2,*** *edited by* Dautray R. and Watteau J.P. (Eyrolles, Paris, 1994), p. 275.

[5] Galmiche D. and Cherfils C. 2002, Hydrodynamic Stability of Indirect-Drive Targets, *in proceedings of the 27th European Conference for Laser Interaction with Matter, Moscow, Russian Federation,* edited by Krokhin O.N., Gus'kov S. Yu. And Merkul'ev Y. A. (The International Society for Optical Engineering, vol. 5228), pp. 28-32